Authors' accepted manuscript. Article published in the *Journal of Surgical Research*, Volume 279, November 2022, Pages 491-504.
The final published version is available at https://doi.org/10.1016/j.jss.2022.05.032

Accepted by Journal of Surgical Research – 2022

Negative in vivo results despite promising in vitro data with a coated compliant electrospun polyurethane vascular graft

Fortin William, MD, MSc[*2,5,6], Bouchet Mélusine, PhD[*1,2,3]; Maire Marion, PhD[1,2]; Héon Hélène, MSc[2]; Ajji Abdellah, PhD[3,4]; Soulez Gilles, MD, MSc[2,6,7]; Therasse Eric, MD[6,7]; Lerouge Sophie, PhD[&1,2,7]

[1]Department of Mechanical Engineering, École de technologie supérieure (ÉTS), Montreal, QC, H3C 1K3, Canada

[2]Research Centre, Centre Hospitalier de l'Université de Montréal (CRCHUM), Montreal, QC, H2X 0A9, Canada

[3]CREPEC, Department of Chemical Engineering, École Polytechnique de Montréal, Montreal, QC, H3C 3A7, Canada

[4]Institute of Biomedical Engineering, École Polytechnique de Montréal, Montreal, QC, H3C 3A7, Canada

[5]Department of Surgery, University of Montreal, Pavillon Roger Gaudry, C.P.6128, Montreal, QC, H3C 3J7, Canada

[6]Department of Radiology, Centre Hospitalier de l'Université de Montréal (CHUM), 1051 Sanguinet Montreal, QC, H2X 0C1, Canada

[7] Department of Radiology, Radiation Oncology and Nuclear Medicine, Faculté de Médecine, Université de Montréal, 2900 Bvd Edouard Montpetit, Montreal, QC, H3T 1J4, Canada

*: Equivalent contribution to the work ; &: Corresponding author

Corresponding author:

Sophie Lerouge, PhD

Research Centre, Centre Hospitalier de l'Université de Montréal (CRCHUM), 900 St- Denis, Montreal, QC, H2X 0A9, Canada

Tel: +1-514-396-8836 || E-mail: sophie.lerouge@etsmtl.ca

Contributions to this work per co-author :

Mélusine Bouchet (MB) and William Fortin (WF) : Co-first authors, study conception, realization of the in vitro (MB) and in vivo (WF) work, data analysis, manuscript writing and revision

Marion Maire and Hélène Héon : Study conception, realization of the in vitro work, manuscript revision

Ajji Abdellah and Éric Therasse : Study conception, manuscript revision

Gilles Soulez : Study conception, realization of the in vivo work, funding, manuscript revision

Sophie Lerouge : Senior author, study conception, funding, realization of the in vitro and in vivo work, data analysis, manuscript revision

ABSTRACT

Background : There is a growing need for small-diameter (< 6 mm) off-the-shelf synthetic vascular conduits for different surgical bypass procedures, with actual synthetic conduits showing unacceptable thrombosis rates. The goal of this study was to build vascular grafts with better compliance compared to standard synthetic conduits and with an inner layer stimulating endothelialisation while remaining antithrombogenic.

Materials and Methods : Tubular vascular conduits made of a scaffold of polyurethane/polycaprolactone (PU/PCL) combined with a bioactive coating based on chondroitin sulfate (CS) were created using electrospinning and plasma polymerization. *In vitro* testing followed by a comparative *in vivo* trial in a sheep model as bilateral carotid bypasses were performed to assess the conduits' performance compared to the actual standard.

Results : *In vitro*, the novel small-diameter (5 mm) electrospun grafts coated with chondroitin sulfate (eVG-CS) showed 10-times more compliance compared to commercial expanded polytetrafluoroethylene (ePTFE) conduits while maintaining adequate suturability, burst pressure profiles and structural stability over time. The subsequent *in vivo* trial was terminated after eVG-CS bypass grafts showed to be inferior compared to their ePTFE counterparts.

Conclusion : The inability of the experimental conduits to perform well *in vivo* despite promising *in vitro* results may be related to the low porosity of the grafts and the lack of rapid endothelialization despite the presence of the CS coating. Further research is warranted to explore ways to improve electrospun PU/PCL scaffold in order to make it prone to transmural endothelialization while being resistant to strenuous conditions.

KEYWORDS

Small diameter vascular graft, electrospinning, surface modification, compliance, *in vivo* study, chondroitin sulfate

1 INTRODUCTION

With ageing of the population and the growing prevalence of coronary and peripheral vascular disease, an increasing number of patients necessitate revascularization procedures [1, 2]. Although many vascular obstructions can be treated by endovascular interventions, surgical bypass grafting remains the only viable option in a large number of cases. In these instances, in the absence of adequate autologous grafts, synthetic conduits are used to bypass the diseased vessel. They reinstate blood flow with acceptable patency rates, as long as the conduit itself possesses an internal diameter greater than 6 mm [3-5]. However, despite significant efforts by several research groups worldwide, there is still no small-diameter (< 6 mm) prosthetic vascular graft showing acceptable patency rates for aorto-coronary and peripheral bypasses [6-11].

Different explanations were given for the failure of synthetic small-diameter bypasses. The lack of significant endothelialization shown by woven polyethylene terephthalate (PET - Dacron) and expanded polytetrafluoroethylene (ePTFE) grafts in humans has been put forward as a crucial point explaining their thrombogenicity [12-15]. Another explanation for bypass graft failure is the low compliance of the synthetic grafts. The compliance mismatch between native and graft material has been shown to promote intimal hyperplasia at the anastomoses and thrombus formation [16-18].

Hence, our hypothesis was that a permanent synthetic bypass conduit promoting endothelialization and with a compliance close to native human vessels could reduce graft failure. Based on these concepts, a novel approach combining electrospinning of polymers and bioactive coatings was developed.

Electrospinning is an alternative process for the fabrication of fiber mats and conduits. It can be used to produce nanofibers structures, either randomly arranged or aligned, and thus create porous scaffolds mimicking the morphology of the extracellular matrix of native vascular structures [19-21, 58]. In this study, we chose to use nanofibers with a diameter around 500 nm based on our previous *in vitro* study showing that electrospun PET (ePET) mats (mean fiber diameter of 550 nm) promoted

the formation of a monolayer of endothelial cells (EC) when compared to conventional woven PET conduit materials where cell invasion through the graft did not favor the formation of a continuous EC layer on their intraluminal surface [22].

More recently, the combination of these mats with a coating made of a thin plasma-polymerized film covered by chondroitin sulfate (CS), a glycosaminoglycan with anti-platelet and pro-endothelial adhesion properties, was shown to promote the formation of a complete and flow-resistant EC monolayer [22-24]. However, electrospun PET still presents low compliance compared to native vessels. To solve this issue, our team hereby introduced an electrospun and similarly coated tubular structure made of a combination of polyurethane (PU) with some polycaprolactone (PCL) (90%/10%). This blend was selected over PET for its better mechanical properties, as it demonstrated a Young's modulus and a compliance closer to that of native arteries compared to other commercial solutions [16, 25-27]. The aim of this study was to produce these electrospun tubular scaffolds, to characterize their structures and mechanical properties as well as stability *in vitro*, and finally to perform a pilot *in vivo* experiment to assess the suturability, patency and endothelialization of these coated electrospun vascular grafts in comparison with commercial ePTFE grafts in a sheep model.

2 MATERIALS AND METHODS

2.1 Grafts production

2.1.1 Materials

PU (polyurethane, MDI-polyester/polyether polyurethane, CAS 68084-39-9), PCL (polycaprolactone, Mn = 80,000), PEO (polyethylene oxide, viscosity average molecular weight Mv = 600,000) and chondroitin sulfate (CS) were purchased from Sigma-Aldrich Canada Co., as well as the chemicals, tetrahydrofuran (THF), N,N-Dimethylformamide (DMF), N-(3-dimethylaminopropyl)-N′-ethylcarbodiimide hydrochloride (EDC), N-hydroxysuccinimide (NHS) and 2-morpholinoethane sulfonic acid (MES). Ethylene (C_2H_4, 99.5 %) and ammonia gas (NH_3, 99.99 %) were obtained from

Air Liquide Canada (Montreal, QC, Canada). A conventional commercially available vascular prosthesis in carbon-coated ePTFE (Impra Carboflo®, 6-mm internal diameter, Bard Peripheral Vascular Inc., Tempe, AZ, USA) was selected as a control.

2.1.2 Electrospinning

PU/PCL tubular scaffolds were fabricated using an electrospinning setup with a 6-mm diameter rotating mandrel. Briefly, a thin layer of a 3 wt% PEO solution was electrospun on the mandrel, followed by the electrospinning of 3.4 mL of a PU/PCL solution (8 wt% consisting of a mix of 90 % PU/10 % PCL (w/w) dissolved in a 1:1 mix of THF and DMF) at a rate of 0.15 $mL.h^{-1}$.The power supply provided a constant voltage of 12 kV between the 21G needle in translation and the rotating drum. Detailed electrospinning parameters were described elsewhere [25]. These electrospinning parameters and the thickness of the scaffolds (~145 µm) were chosen based on previous work [25] showing that this thickness enables to get adequate impermeability and burst resistance, as well as good handling properties. At the end of the process, the mandrel was immersed in EtOH 50 % in order to dissolve the PEO layer and to retrieve the electrospun vascular graft, hereafter called eVG.

2.1.3 Coating preparation (Plasma-polymerization followed by Chondroitin-Sulfate grafting)

The coating was created as already described in detail [23, 24]. First, a thin layer of primary amine-rich coating, designated as L-PPE:N, was deposited through plasma deposition on the surface of the grafts in a low-pressure capacitively coupled radio frequency (r.f., 13.56 MHz) glow discharge plasma reactor using ethylene (C_2H_4) and ammonia (NH_3) with flow rates of 20 sccm and 15 sccm respectively. The deposition was performed at 80 Pa pressure under mild conditions (power, P=15W) during 15 minutes to form a coating of about 100 nm thickness.

After inside-out turn of the prosthesis, CS was covalently grafted on amine groups via a carbodiimide chemistry (EDC/NHS), as previously reported [28]. In brief, the tubular scaffolds were immersed in a solution containing 0.01 g.mL-1 CS, 40% v/v EtOH, 50 mM MES, 22.8 mM EDC and 4.6 mM NHS during 1h at room temperature before rinsing once with PBS and twice with Milli-Q water. The final product is hereafter called eVG-CS.

2.1.4 Grafts preparation for *in vivo* tests

All prostheses were cut to a 7cm-length. The ePTFE prostheses were prepared under sterile conditions under a hood and kept in a closed sterile pouch until use. eVG-CS were wrapped in peel pouches and sterilized by V-PRO maX low temperature system (Steris).

2.2 In vitro characterization

2.2.1 Composition, morphology and permeability

Fiber morphology was determined by scanning electron microscopy (SEM; TM3030Plus instrument, Hitachi, Tokyo, Japan) after deposition of a 20 nm-thick layer of chromium conductive coating. Diameters were measured through ImageJ software (NIH, USA) analysis, based on about 200 different fibers. Pore size was calculated for ePTFE and eVG-CS materials.

The CS grafting on eVG was verified through the analysis of surface composition by X-Ray Photoelectron Spectroscopy (XPS). Surveys (0-1200 eV) were acquired normal to the surface with a VG ESCALAB 3MkII instrument, using nonmonochromatic Mg Kα radiation. Charging was corrected by referencing all peaks with respect to the carbon (C 1s) peak at binding energy of 285.0 eV. Quantification of the constituent elements was performed using Avantage v5.979 software (Thermo Fisher Scientific Inc., Waltham, MA, USA) after Shirley-type background subtraction. Since CS

contains sulfate groups, atomic concentrations of sulfur were determined at the samples surfaces to confirm the grafting, in comparison with uncoated samples.

The chemical composition of electrospun scaffolds was also characterized by attenuated total reflectance Fourier transform infrared (ATR-FTIR) spectroscopy (Spectrum GX, PerkinElmer, Waltham, MA, USA). All spectra were taken in the spectral range by the accumulation of 32 scans with a resolution of 4 cm^{-1}, and were compared to the spectra of pure PU and PCL pellets. At least three samples were analyzed for each condition.

Permeability testing on the eVG-CS grafts was done in order to ensure blood transudation through the prosthesis walls was acceptable. It was quantified by fitting the grafts in a BioDynamic® chamber of an ElectroForce® 3200 (TA Instruments, New Castle, DE, USA) and connecting them to a water flow system. Water pressurized at 120 mmHg was circulated to the grafts and the fluid permeating through their walls was collected for 15 minutes. The water permeability was calculated according to the ANSI 7198 standard [29], using the equation: $Pw = Q/A$, where Pw is the water permeability of the tubular scaffold (expressed in $mL.cm^{-2}.min^{-1}$), Q is the flowrate of the permeated volume during the test and A is the graft area allowing the permeation in the sample holder.

2.2.2 Mechanical Characterization

A uniaxial tensile testing machine (ElectroPuls™ E3000, Instron®, Illinois Tool Works Inc., Norwood, MA, USA) equipped with a 250 N load cell was used for evaluating tensile properties in the circumferential direction, as well as the suture retention strength.

Tensile tests were performed according to the ASTM D882-12 [30], with some modifications. The initial gage length was set to 4.5 mm and the strain rate was of 10 %/min. eVG-CS were cut into rectangular samples in the longitudinal direction and strips with a 5 mm width from at least four different samples were tested. Elastic modulus and tensile strength were calculated through engineering stress-strain curves.

The suture retention strength was determined using strips of eVG-CS with a 15 mm width. The sample was threaded with 7-0 Prolene® Polypropylene suture (Ethicon US, LLC, Cincinnati, OH, USA) at 2 mm from its edge. The suture was pulled at a constant rate of 100 mm/min parallel to the longitudinal axis of the prosthesis. The suture retention strength is defined as the force required to pull a suture from the prosthesis or cause the wall of the prosthesis to fail [29], namely the peak force obtained during this procedure. At least three different samples were tested for each test.

2.2.3 Ageing

To evaluate possible degradation of the constitutive material of the grafts, bare electrospun tubular scaffolds were kept at 37°C in a saline solution during 1, 3 and 6 months. At each time point, the following characteristics were measured: fiber diameters, elastic modulus in the circumferential direction, chemical structure (ATR-FTIR), as well as the graft weight (NewClassic MF Analytical Scale balance with 0.1 mg resolution, Mettler-Toledo Inc., Colombus, OH, USA) after drying.

2.3 In vivo implantation

2.3.1 Study design

In this study, experimental coated electrospun grafts (eVG-CS) were compared with commercially available ePTFE prostheses. Both grafts were implanted as bilateral end-to-end common carotid bypasses in ten sheep, ePTFE graft serving as a control. Each conduit's (experimental or ePTFE) implantation side (left or right common carotid artery) was randomly selected at the beginning of the study.

2.3.2 Animal selection and care

The sheep was selected for this study because of its suitable target vessels diameters (common carotid, 5-7 mm) for small-diameter vascular graft implantation and its coagulation system resembling most the human's when compared to other large animals [31]. Animal surgical procedures and follow-up studies were approved by the institutional animal care committee at the Centre de recherche du Centre Hospitalier de l'Université de Montréal and the Canadian Council on Animal Care. The study was conceive accordingly to the ARRIVE guidelines [32]. Ten mixed breed (Polled Dorset cross Rideau Arcott, Alpha Ovine, Norwood, ON, Canada) female sheep (26-39 Kg) were used in this study. All animals were kept in acclimation at least one week prior to graft implantation.

2.3.3 Surgical protocol

Each animal was given 80 mg of acetylsalicylic acid (Pharmascience Inc., Montreal, QC, Canada) per day for three days preoperatively. After overnight fasting, the sheep were led to the operating theater. Complete anesthesia protocol is available in the supplemental material section (Appendix B).

Surgical exposition of both common carotid arteries was led via a single longitudinal median neck incision. The left carotid artery was systematically approached first and dissected over a 7-cm segment. Heparin (250 Units/Kg, Heparin USP, Sandoz, Boucherville, QC, Canada) was given intravenously 2 to 5 minutes prior to carotid clamping. Following resection of a 5.5 cm long carotid segment, the randomly selected 5.5-cm long vascular graft (eVG-CS or ePTFE) was anastomosed in an end-to-end fashion, using 7-0 polypropylene running sutures. Flushing of the neo-conduit was done via a 26-gauge needle before definitive reestablishment of blood flow. Implantation of the contralateral graft was done in a similar fashion. After careful hemostasis, closure of the wound was done in a conventional manner. Both implanted grafts are shown on **Figure 1**.

Each sheep received low-molecular-weight heparin (40 mg, Enoxaparin sodium solution, Lovenox®, Sanofi-Aventis Canada Inc., Laval, QC, Canada) every day for three days post-operatively and were then given acetylsalicylic acid (80 mg) every day until the end of the study.

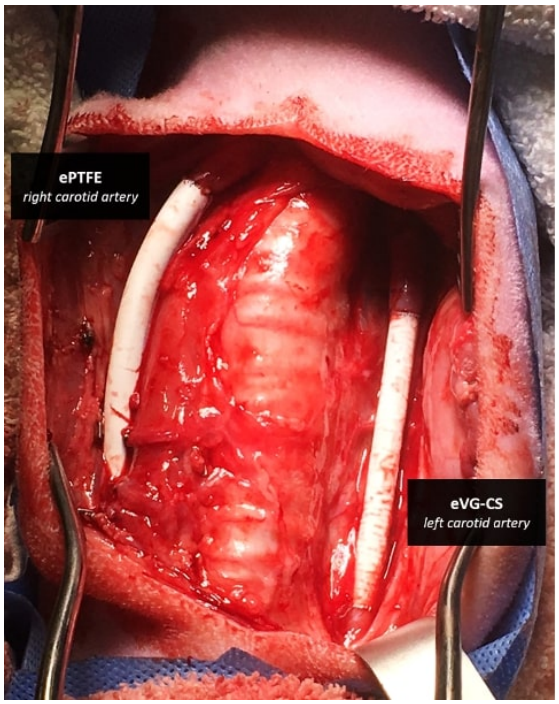

Figure 1 - *In vivo* implantation of eVG-CS and ePTFE grafts as bilateral carotid bypass.

2.3.4 Ultrasonographic follow-up

A duplex ultrasonographic study was performed preoperatively on the first sheep for baseline information on velocities, and a standardized echographic follow-up protocol was planned on each graft at different timelines: immediately post-operative, at 1 week, 4 weeks, 8 weeks and 12 weeks (prior to sacrifice). Peak systolic velocity and ratio measurements were measured systematically on five different sites, including the perianastomotic segments.

2.3.5 Animal sacrifice and graft analyses

Sheep were euthanized by IV sodium pentobarbital (108 mg/kg, Euthanyl Forte, Bimeda-MTC Animal Health Inc., Cambridge, ON, Canada). Before harvesting, prostheses were infused with a saline solution for 5 minutes, followed by a formalin solution for 5 minutes. In case of occluded grafts, no irrigation was performed in order not to disrupt the intraluminal content. All explants (20; 10 eVG-CS,

10 ePTFE) were analysed qualitatively for macroscopic appearance, then were immersed in a formalin solution and stored at 4°C. Each graft was subsequently cut into different axial and longitudinal sections, then embedded in paraffin and stained with hematoxylin phloxine saffron (HPS).

2.3.6 Study termination

The study was terminated nine weeks after its initiation, following several duplex ultrasound follow-up results showing poor patency of the experimental grafts compared to ePTFE controls.

2.4 Statistical analysis

Statistical tests were carried out through GraphPad Prism Software Version 7.0 (San Diego, CA, USA). Normality was tested using D'Agostino-Pearson normality test and unpaired t tests with Welch's correction were performed when comparing two groups only. Data are then expressed as the mean ± SD. When the number of samples was small (mechanical tests), Kruskall-Wallis's non parametric tests were performed and data are expressed in the form of Boxplots with median and interquartile range. A Fisher's test was used to compare the *in vivo* patency of both prostheses. P values of less than 0.05 were considered significant.

3 RESULTS

3.1 In vitro characterization

Electrospun grafts were observed by SEM and showed nanofibers with a random orientation (**Figure 2**) and a mean diameter of 523 ± 93 nm in the bare state. No significant difference was observed after the addition of the coating on the grafts (533 ± 57 nm, p = 0.08). The mean pore diameter was evaluated at 1.8 ± 0.8 µm with the fitting ellipse method (the average for the major axis and the minor axis are respectively 2.4 ± 0.7 µm and 1.2 ± 0.4 µm). The thickness of eVG-CS mats was 148 ± 23

µm, while ePTFE grafts were almost 5-fold thicker with an average wall thickness of 692 ± 28 µm. In ePTFE grafts, a typical node-fibril microstructure was observed with internodal distances, described as pore size [33], of 17 ± 6 and 20 ± 7 µm for the inner and outer layers, respectively.

An average sulfur concentration of 1.3 ± 0.2 % was measured at the surface of coated electrospun grafts though XPS technique, while no sulfur was found on bare grafts. This was consistent to previous results on electrospun PET [24, 34] and confirmed the presence of CS at the intraluminal surface of eVG-CS.

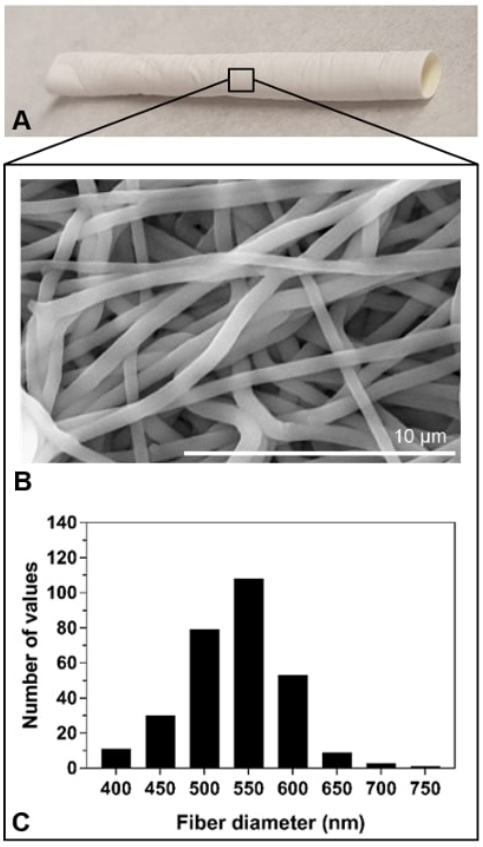

Figure 2 - (A) Digital image of the graft. (B) SEM image of the nanofiber mat from eVG nanofiber mat (scale bar: 10 µm). (C) Distributions of fiber diameters for coated grafts. There was no difference between bare and coated materials.

Tensile testing of circumferential samples of eVG and eVG-CS demonstrated their quite linear elastic behavior until rupture (**Figure 3**), with a similar Young's modulus (4.6 ± 0.9 MPa and 4.7 ± 1.0 MPa

for bare and coated materials, respectively). eVG-CS exhibited a slightly higher tensile strength compared to eVG mats (14.3 ± 2.8 MPa and 10.0 ± 1.7 MPa, respectively, p = 0.04).

These values are close to those found in our previous study for bare eVG (mean E = 3.9 ± 0.4 MPa) for which the compliance was measured to be of 0.0360 ± 0.0018 %/mmHg at the 80-120 mmHg pressure range [25]. As the compliance is correlated with the elastic modulus [36], we can expect the compliance of eVG-CS to be in the same order of magnitude. In contrast, ePTFE grafts exhibit higher Young modulus (17.4 ± 1.8 MPa, Figure 3B) and about 10 times lower compliance (0.0033 ± 0.0005 %/mmHg [25], 0.0026 ± 0.0009 %/mmHg [35]).

Suture retention strength was measured in the longitudinal direction with an average value of 2.72 ± 0.56 N (min-max: 2.03-3.88 N). This is higher than the generally accepted threshold value for implantation, namely 2 N [37]. Besides, as for bare grafts [25], eVG-CS presented a very low water permeability, below 0.002 $mL.cm^{-2}.min^{-1}$, meaning that the addition of the CS hydrophilic coating on the lumen surface of prostheses didn't increase their permeability.

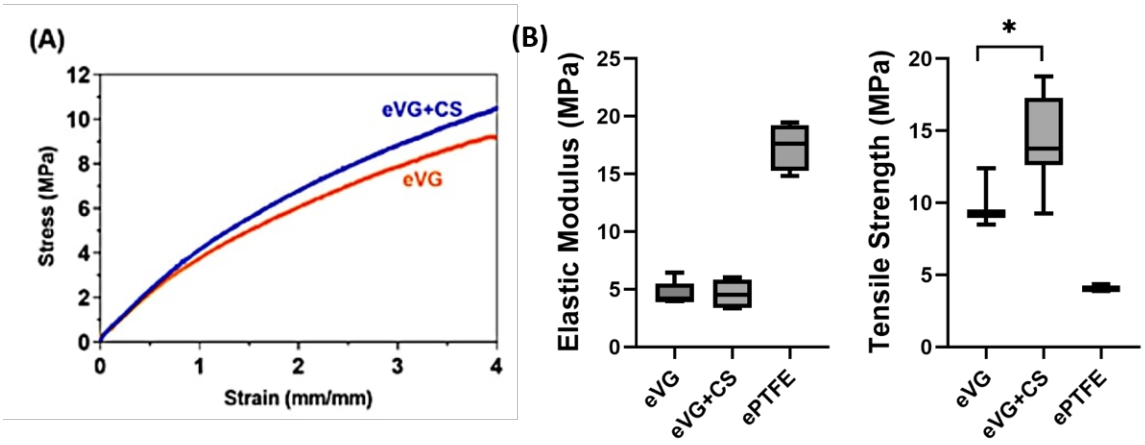

Figure 3 - Mechanical properties of eVG and eVG-CS grafts. (A) Representative engineering stress-strain curves from circumferential tensile testing. (B) Boxplot of the elastic modulus and tensile strength, in comparison to ePTFE grafts (n=13; * p<0.05).

No discernable weight loss was detected through 6-month ageing of electrospun mats in saline, as well as no changes in their morphology and in the distribution of fiber diameters (See Appendix A). Tensile tests also showed that the elastic modulus and the tensile strength of eVG remained stable during the 6-month ageing period (**Figure 4A**). FTIR analysis confirmed the presence of both PU and PCL in the electrospun PU/PCL scaffolds. No differences were observed between spectra taken over the 6-month ageing period (**Figure 4B**).

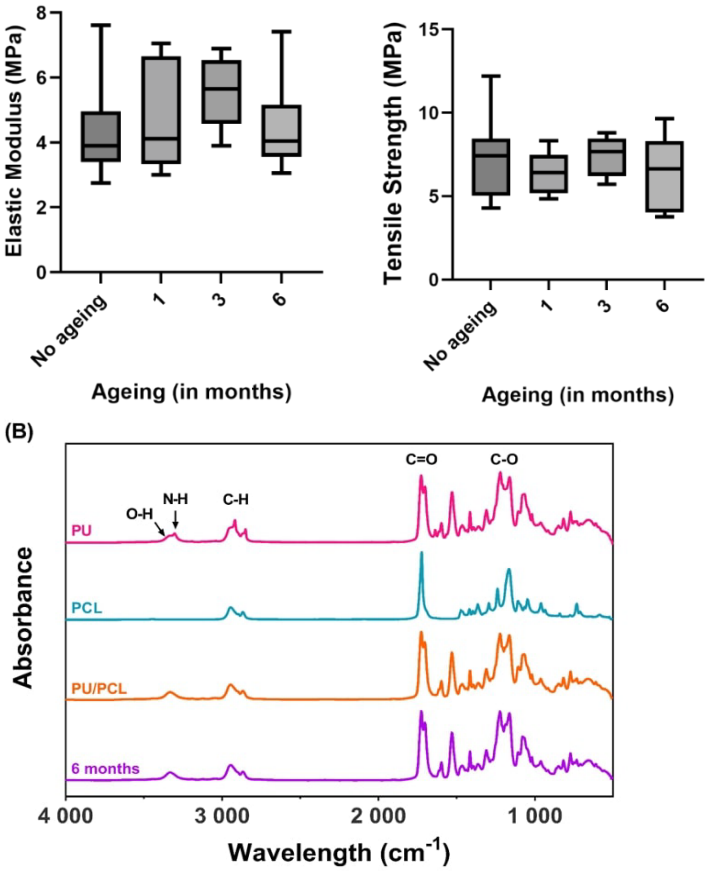

Figure 4 - Comparison of (A) the elastic modulus and the tensile strength of the eVG scaffolds as a function of ageing duration in a saline solution at 37°C over 6 months, and (B) ATR-FTIR spectra of pure PU, pure PCL and eVG scaffolds after production and after 6-month ageing. Functional groups of –CH2 (stretching) and carbonyl keton –C=O (stretching) were detected in the ranges of 2850-3000 and 1670-1750 cm^{-1} for all spectra. The hydroxyl –O-H (stretching) and –N-H (stretching) from PU were identified to the broadened peak in the range 3200-3400 cm^{-1} and were also detected in the PU/PCL spectrum. No difference was observed between fresh and aged PU/PCL samples.

3.2 In vivo operative outcomes and animal management

A total of 10 sheep were operated as per protocol. Mean carotid cross clamp time was significantly lower for eVG-CS grafts compared to ePTFE grafts (46.6 ± 12.5 minutes vs 60.0 ± 8.0 minutes, $p < 0.001$), probably due to the ease of handling and suturability of the thin electrospun grafts. All grafts were successfully anastomosed to their intended native carotid artery and were free from any visual defect at the time of wound closure.

Three sheep were euthanized or died in the immediate postoperative period - one from per-operative cerebral anoxia attributed to persistent desaturation at the time of carotid cross clamping, and two from respiratory distress attributed to a laryngeal dysfunction secondary to cervical dissection. One sheep was sacrificed at 4 weeks after surgery secondary to persistent respiratory obstruction, and the remaining six sheep were sacrificed at 5-to-8 weeks after surgery (see **Table 1**), at the time of the termination of the *in vivo* study.

Table 1 - *In vivo* follow-up results. Time *in vivo*: time from implantation to animal sacrifice.

Animal #	**Carotid with eVG-CS graft**	**Time *in vivo* (weeks)**	**eVG-CS at sacrifice**	**ePTFE at sacrifice**
1	Right	< 24h	Patent	Patent
2	Left	7	Stenosis	Patent
3	Right	7	Occlusion	Patent
4	Left	7	Stenosis	Patent
5	Left	5	Occlusion	Patent
6	Left	4	Patent	Patent
7	Right	< 24h	Patent	Patent
8	Right	8	Stenosis	Patent
9	Right	8	Patent	Patent
10	Right	< 24h	Patent	Patent

3.3 Ultrasonographic baseline and follow-up data

All 10 animals underwent immediate post-operative duplex ultrasound as per protocol, and all eVG-CS grafts were patent and free from any apparent thrombus or stenosis. Doppler signal was absent in ePTFE grafts in the immediate postoperative period, because of the attenuation of the ultrasound in the graft wall [38], but graft patency and freedom from significant stenosis was confirmed by antegrade flow and normal distal common carotid artery velocities on the immediate post-operative duplex ultrasound examination. All grafts became echogenic at subsequent examinations and were analyzed as per protocol.

Seven animals underwent subsequent follow-up duplex ultrasounds 4 to 8 weeks postoperatively until study termination. At one week, all ePTFE and eVG-CS grafts were patent and free from stenosis. On final ultrasounds prior to sacrifice of the animals that underwent follow-up studies, five out of the seven (71 %) remaining eVG-CS grafts showed either mural thrombus, significant stenosis or complete vessel occlusion, while none (0 %) of the seven ePTFE grafts showed any sign of stenosis or thrombus adhesion ($p = 0.021$) (**Table 1**, **Figure 5**).

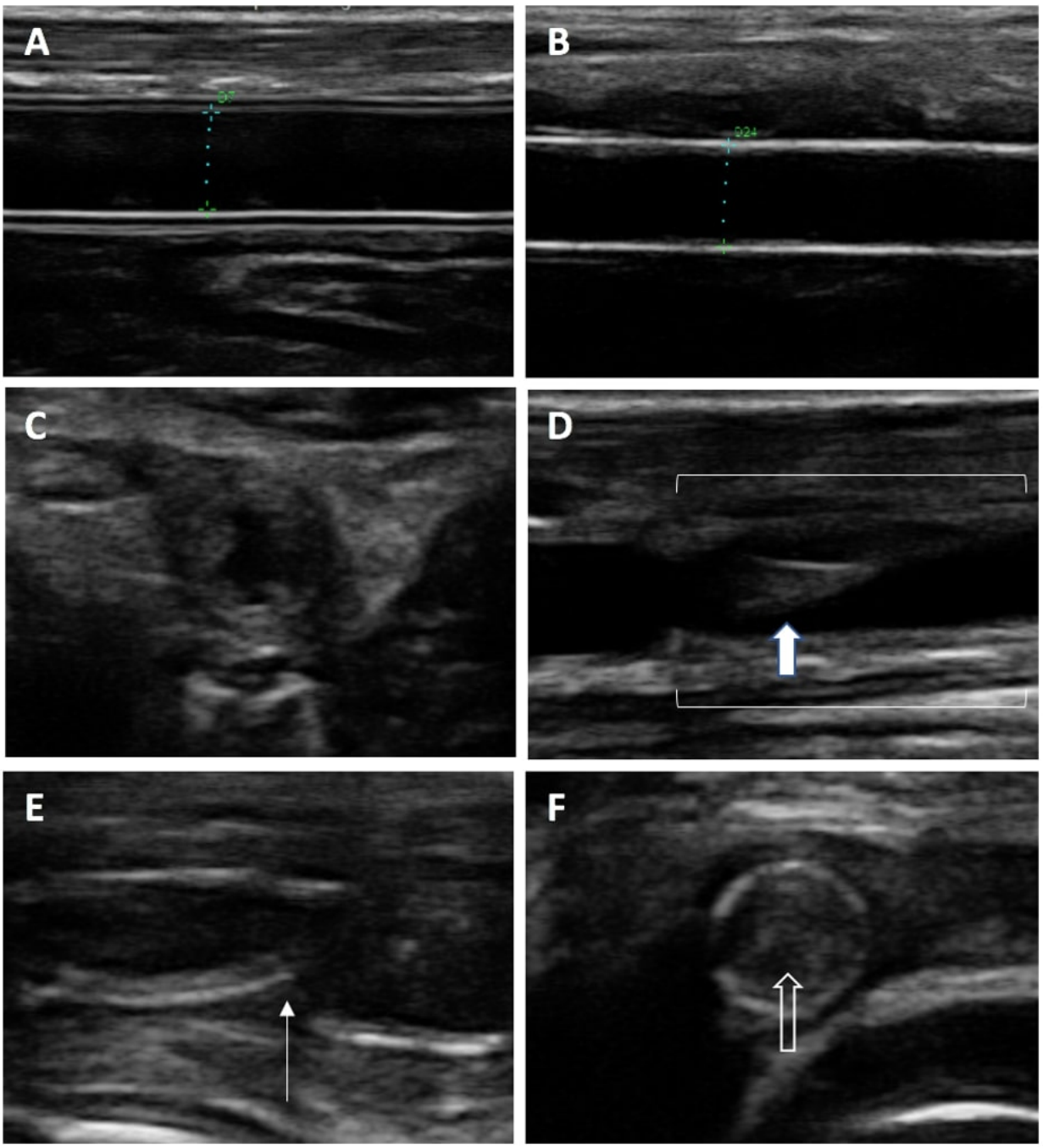

Figure 5 – Ultrasonographic in vivo analyses. Longitudinal representations of patent ePTFE (A) and eVG-CS grafts (B) prior to sacrifice (intima-to-intima distance represented by dotted lines). (C) Axial depiction of adherent mural thrombus formation leading to stenosis at 4 weeks in an eVG-CS graft. (D) Longitudinal image of neointima detachment (large arrow) in an eVG-CS graft (delimited with boxes) at 7 weeks, suggesting weak attachment of the neointima to the luminal side of the graft. (E) Apparent plicature (thin arrow) of an eVG-CS graft that led to subsequent thrombosis at 4 weeks (sheep #5). (F) Occlusion of an eVG-CS graft at 4 weeks with dense thrombus formation within the prosthesis (empty arrow).

3.4 Macroscopic analyses and histological examinations

All twenty prostheses were harvested and analysed as per protocol. Macroscopic analysis of grafts that were explanted a few hours after surgery (6 grafts, 3 eVG-CS and 3 ePTFE) demonstrated the permeability and the absence of any major trauma of all conduits. Macroscopic analysis of conduits that were kept *in vivo* for 4 weeks or more (14 grafts, 7 eVG-CS and 7 ePTFE) showed that ePTFE grafts systematically exhibited higher rigidity and increased adherence to surrounding tissues when compared to eVG-CS grafts (**Figure 6**).

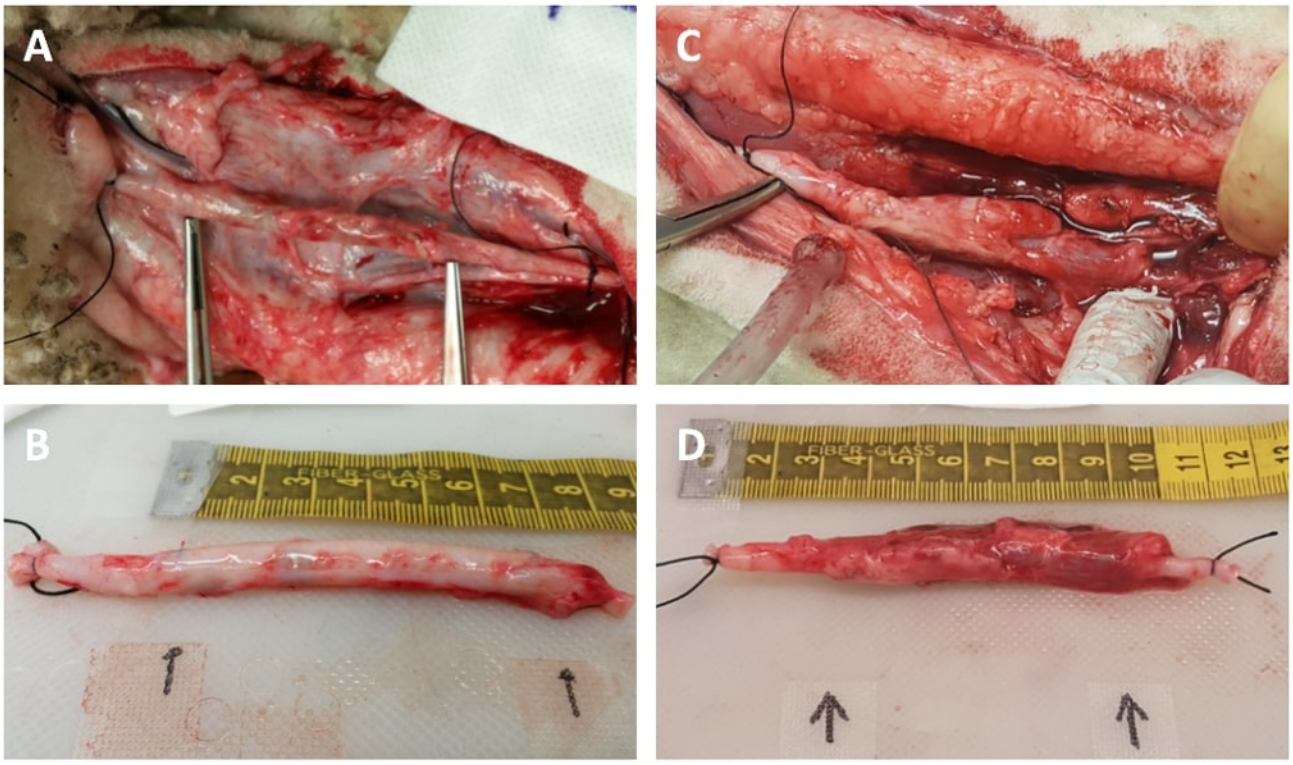

Figure 6 - Macroscopic analysis. Typical macroscopic appearance of (A, B) eVG-CS grafts after 8 weeks *in vivo*, (C, D) ePTFE prostheses after 5 weeks *in vivo*, showing more tissue adhesion around ePTFE grafts.

Figures 7 and **8** summarize the histological observations for ePTFE and eVG-CS, respectively. Histological analyses performed on the 6 grafts that were explanted a few hours after surgery

confirmed the patency and absence of any major structural trauma on either eVG-CS or ePTFE conduits. However, analysis of the grafts that were kept *in vivo* for 4 to 8 weeks confirmed the formation of thrombus that led to stenosis or occlusion in 5/7 eVG-CS grafts (**Fig. 8E,F**), while the all ePTFE grafts presented good patency with only few intraluminal thrombus.

Two other major differences were noticed between histological slides from eVG-CS or ePTFE conduits. One of them is the presence of cells throughout the wall of ePTFE grafts (**Fig. 7A, B)**, while no cells were observed within the thickness of the eVG-CS graft (**Fig. 8B**). In addition, while the rounded morphology of ePTFE was preserved on transverse sections (**Fig. 7A)**, it was not the case for some eVG-CS, most probably due to lower radial force in the latter (**Fig. 6**). Moreover, most eVG-CS grafts exhibited different degrees of structural degradation on large parts of the conduits' walls (**Fig. 8 E,F**).

Morphometric analysis was attempted on grafts that were kept *in vivo* for 4 weeks or more, but the occlusion or degradation of the eVG-CS conduits was too important for a definitive comparison of the extent of graft covered by neointima. Some eVG-CS grafts showed neointimal proliferation on the perianastomotic area of their intraluminal aspect (**Fig. 8A**), but only over a few millimeters or centimeters, which was similar to the degree of endothelialization observed in ePTFE grafts. Besides, there was no strong cohesion between the neointima and the electrospun materials. **Figure 8C** (corresponding to ultrasound image in Fig. 6D) shows an example of neointima detachment from the graft surface at the distal side of eVG-CS that led to the formation of a sub-endothelial blood clot and subsequently to the graft occlusion. In contrast, cell invasion inside the porosities of ePTFE was obvious, leading to a more adherent peri-anastomotic neointima (**Fig. 7D**).

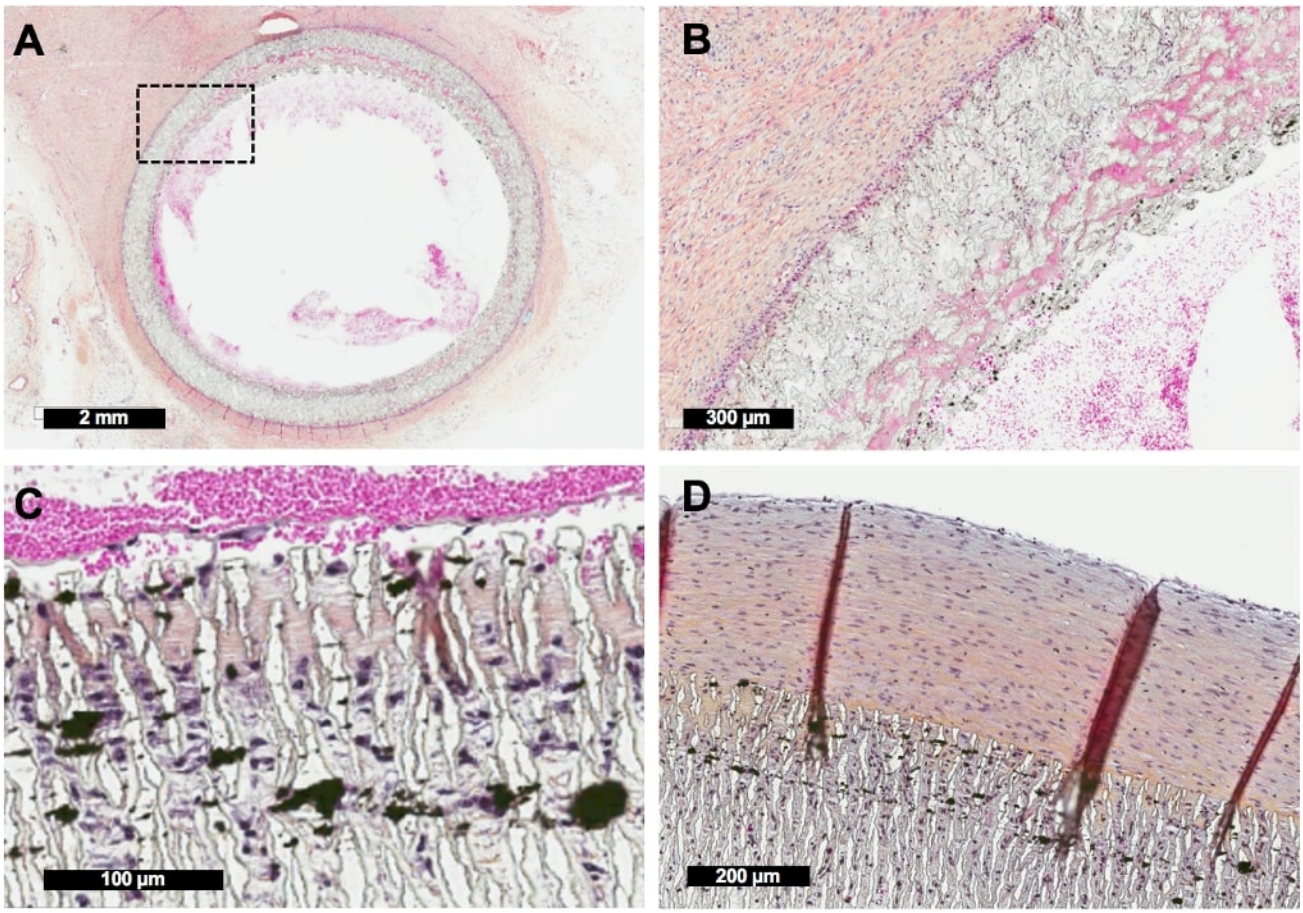

Figure 7. Control ePTFE graft after severeal weeks implantation shows well attached neointima at anastomosis sites but not throughout the length of the implant. (A, B insert): Typical transverse section in the middle of ePTFE implant, showing some intraluminal thrombus, invasion of the graft by plasma, and cells, and a large amount of perigraft tissue around the implant (sheep #2). (C) Longitudinal section showing cell invasion through the ePTFE porosity (black spots are carbon from the prosthesis). (D) Strong neointima attachment close to the anastomosis (HPS staining).

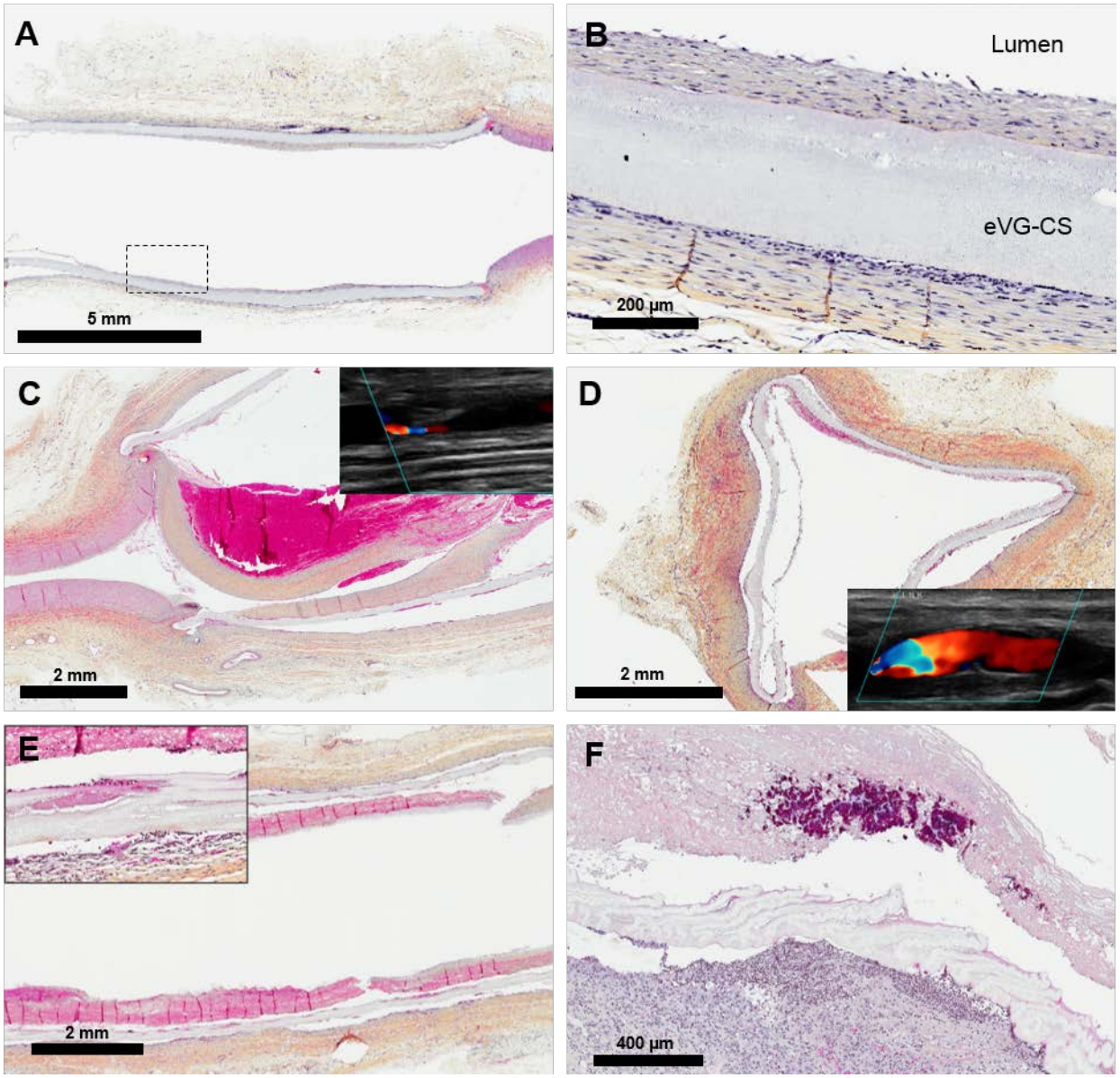

Figure 8. Histological analyses of experimental PU/PCL grafts after several weeks of implantation. (A, B insert): Example of patent eVG-CS graft after 8 weeks implantation: distal anastomosis, with thin neointima limited to the perianastomotic area and complete absence of cell invasion within the electrospun VG (sheep #9). (C) Detachment of the neointima from the prosthesis in the anastomosis region led to the formation of a sub-endothelial thrombus, which was visible by duplex ultrasounds (sheep #2). (D) The lower radial force exerted by eVG-CS grafts, confirmed by their deformation during histological sectioning, can lead to kinking and flow disturbance. (E, F) Thrombosed eVG-CS grafts showed major structural deformations, ranging from intra-wall deficits to frank fiber separation (sheep #6 and #3). (HPS staining).

4 DISCUSSION

Electrospinning has been the source of increasing interest in the past few decades in the process of creating novel vascular grafts [19-26, 44, 47, 54-56]. This technique notably offers the possibility to control the structure, the composition and the mechanical properties of the vascular scaffolds. The goal of this work was to evaluate a proposed optimal combination of a compliant vascular scaffold with an internal coating to achieve enhanced permeability and anti-thrombogenicity of novel small-diameter vascular grafts.

The CS coating has been previously studied in vitro and demonstrated to reduce protein absorption significantly (in particular fibrinogen, known to induce thrombosis) and platelet adhesion to a similar level that PEG low-fouling surfaces [23]. It was also shown to enhance the adhesion, growth and retention endothelial cells seeded on the surface under flow when compared to bare PET grafts commonly used for vascular grafts. It therefore appears as a very promising coating for vascular grafts. In this work, a similar coating was created on small-diameter electrospun PU vascular conduits. These were first characterized *in vitro* then implanted *in vivo* in 10 sheep. *In vitro* tests confirmed the integrity of the electrospun conduits and the grafting of the coating to their internal scaffold. Experimental conduits displayed a compliance about 10-times higher than commercially available ePTFE vascular conduits and an adequate suturability profile. Six (6)-months ageing tests in a 37°C saline solution also suggested that, as expected, the experimental conduits do not undergo significant degradation with time, at least in short term and under static conditions.

In the *in vivo* portion of our study, the electrospun conduits were compared to commercially available ePTFE vascular grafts as bilateral interposition carotid bypasses in a sheep model. This relatively new model has been previously described by Jirofti et al. [55] for the application of an electrospun PCL/PU graft as a vascular carotid bypass graft in sheep. The mean diameter of the fibers was similar to ours (around 400 nm) but in contrast to the PU/PCL mix, the authors used co-electrospinning to combine fibers of 15% PCL with fibers of 10% PU. They could ultimately show patency of 5-mm diameter, 3-

cm long PCL/PU graft in 9 sheep up to 32 weeks after implantation, which confirms the adequacy of the present animal model. ePTFE was chosen as a reference here since it presents good patency rate but poor endothelialization due to the inertness of the material. Although surgical implantation was mostly uneventful, four sheep out of ten suffered from respiratory complications related to the surgical approach and had to be sacrificed immediately (3 sheep) or earlier than expected (1 sheep at 4 weeks). These complications could be explained by the use of a ventral sagittal surgical approach, with a single midline incision over the trachea. To expose each carotid artery, the trachea had to be moved laterally. This may have induced tension on surrounding tissues resulting in swelling and inflammation. It appears that sheep are prone to inflammation and swelling when tissue of the cervical region are manipulated. A bilateral approach, by creating two incisions on each side of the trachea, should be preferred to reduce tissue trauma. These complications, although unexpected, allowed us to gather invaluable information on the experimental conduits' behavior in the animals over time. Of important note, all selected sheep were of female gender, due to institutional and health concerns. Indeed, Q Fever is an endemic disease in sheep and represents a significant safety hazard if contracted by humans, particularly pregnant women. Animal selection for this study was not gender-based by definition, but driven by the ability of a provider to ensure the animals were exempt of this disease to protect our veterinarian caregivers. Only one medical-grade ovine provider in the country could confirm our team that their sheep were systematically tested for Q-fever and this company only provided female individuals. Hence, although involuntary, this gender bias has to be taken into account when interpreting the results of this study.

The study on the remaining sheep was terminated at nine weeks, after duplex ultrasound follow-up showed inferiority of the experimental conduits. Different hypotheses could explain the inferiority of the experimental conduits compared to ePTFE grafts *in vivo* even though they had shown promising results in the *in vitro* phase. Five out of the seven eVG-CS grafts that remained *in vivo* for 4 to 8 weeks presented significant thrombus formation or complete thrombosis. Those grafts were also the ones

that showed physical degradation or kinking, while the two physically intact grafts were free from any clot formation. This observation could suggest that the grafts themselves were not inherently thrombogenic in their intact form but may have gained this characteristic with time. A possible reason for that is that to obtain the coating on the luminal side of the eVG grafts, a manual processing step of inside-out turn for each prosthesis was required after plasma deposition. This might have inflicted surface default and micrometric damages through prosthesis wall, or exposed the underlying thrombogenic L-PPE:N coating, leading to increased thrombogenicity. A solution to that would be to create the amine-rich layer coating directly inside the eVG, either by using plasma reactors with cylindrical configuration [39, 40], or by the use of other wet chemical techniques such as the introduction of amine groups by an aminolysis reaction [41, 42].

The smaller radial force exerted by the eVG-CS could also increase the propensity of the eVG to collapse or kink during flexions and hyperextensions seen in large animals and in many human anatomical positions (knee, neck etc.). While its importance in the present study cannot be asserted, mechanical tests reproducing these conditions should be performed. The design of eVG could be modified to provide higher radial force by playing on the orientation of fibers or to provide a higher kink resistance like by pleating the grafts [56].

Another important point to discuss is the fact that the two intact experimental grafts that remained *in vivo* for 4 and 8 weeks respectively showed adequate incorporation and neointimal formation on the peri-anastomotic area but did not display improved endothelialization further in the middle of the graft compared to the ePTFE controls. This is likely to be due to the small pore size of the eVG grafts. We chose such a low porosity based on some previous *in vitro* research showing the formation of a complete endothelial monolayer with cell-cell contact [22, 46, 47] in contrast to structures with large pores where cells penetrate into the structure and are less likely to form a complete endothelial barrier [22, 46, 48]. However, the absence of cell invasion within the graft also has two drawbacks. First, on the luminal surface, it limits the anchorage of neointimal tissue, as it could be observed here with

cases of neointima detachment from the grafts. Second, it limits the formation of perigraft tissue and capillary ingrowth though the graft, which is believed to play an important role in transmural endothelialization.

Indeed, neo-endothelialization develops via three mechanisms: transanastomotic ingrowth, transmural migration and seeding from circulating endothelial cells progenitors [6, 15, 33, 49, 51]. The transanastomotic ingrowth was identified as the more probable endothelialization mechanism in most animal studies [15]. However it is generally restricted to the first 1-2 cm around the anastomoses [6, 15, 49], as it is observed in the case of our study, and is even more limited in humans [50]. Another mechanism is transmural endothelialization arising from the capillary ingrowth of perivascular tissue through the pores of the graft wall [15, 33, 51]. Transmural growth has been described to occur significantly faster on high-porosity grafts [49, 52-54, 57]. Zhang et al. thus compared PU prostheses of two porosities and concluded that the rapid ingrowth of perigraft collagenous tissue in the most porous prostheses may have accelerated the lining of endothelial-like cells [49]. In the present case, the very low porosity clearly prevents the contribution of transmural migration to the neo-endothelialization of the conduit. Building a more porous vascular PU/PCL scaffold could be a way to encourage endothelial migration through this mechanism [49, 52, 54].

In contrast to PU/PCL grafts, ePTFE grafts are much more porous and showed pronounced cellular invasion throughout the graft thickness, with obvious communications between the perigraft tissue and the graft lumen and better adhesion of the neointima when present. However, the neointima was still incomplete at 8 weeks, apart from the anastomotic regions, in accordance to other animal studies [6, 49]. This shows that while probably necessary, high porosity is not sufficient to induce a complete neoendothelium on the luminal surface of the graft. This is why the CS bioactive coating was being tested here as a potential strategy to improve the neoendothelialization and patency rate of small diameter vascular grafts. This coating had been shown *in vitr*o to enhance the adherence and resistance to flow of endothelial cells pre-seeded on scaffolds [22]. However, in this study, endothelial

cells were not pre-seeded, and the absence of better endothelialization on the two intact experimental CS-coated graft suggests that the CS coating was not able to enhance endothelial cells deposition through the rapid recruitment of circulating endothelial progenitor cells, the third known endothelialization process described in the literature [33, 51]. No in vitro model could perfectly reproduce the various biological mechanisms in competition with endothelial cell attachment under flow in the presence of blood and smooth muscle cells. This highlights the importance of rapid in vivo testing to promptly assess the potential and limitations of any new implantable device or material.

5 CONCLUSION

This study portrays the building and pilot *in vivo* testing of small-caliber nanofibrous electrospun PU/PCL vascular grafts coated with a chondroitin bioactive coating. The grafts showed promising behaviors in terms of compliance and suturability and did not show deterioration over a 6-month period in *in vitro* settings. However, the grafts did not perform as expected in strenuous *in vivo* settings, and further research is warranted to explore possible improvements to the scaffold's porosity and coating to increase their likeliness to induce a stable, homogenous neo-endothelium.

ACKNOWLEDGEMENTS

This study was jointly supported by the Canada Institutes of Health Research (CIHR) and the Canada Research Council in Natural Sciences and Engineering (NSERC) (Collaborative Health Research Projects CPG 127764) and Lerouge's Canada Research Chair in biomaterials and endovascular implants (CRC, 950-229036). M. Bouchet gratefully acknowledges scholarships from École de technologie supérieure. The authors also thank the team of Pr. M. Wertheimer and G. De Crescenzo, as well as M. Gauthier (École Polytechnique), M. Gouin, B. Chayer and I. Salazkin (CRCHUM) and the personnel of the CRCHUM Animal core facility for their collaboration in the project and their skilled technical support.

CONFLICT OF INTEREST

None to declare.

APPENDIX A. Supplementary data

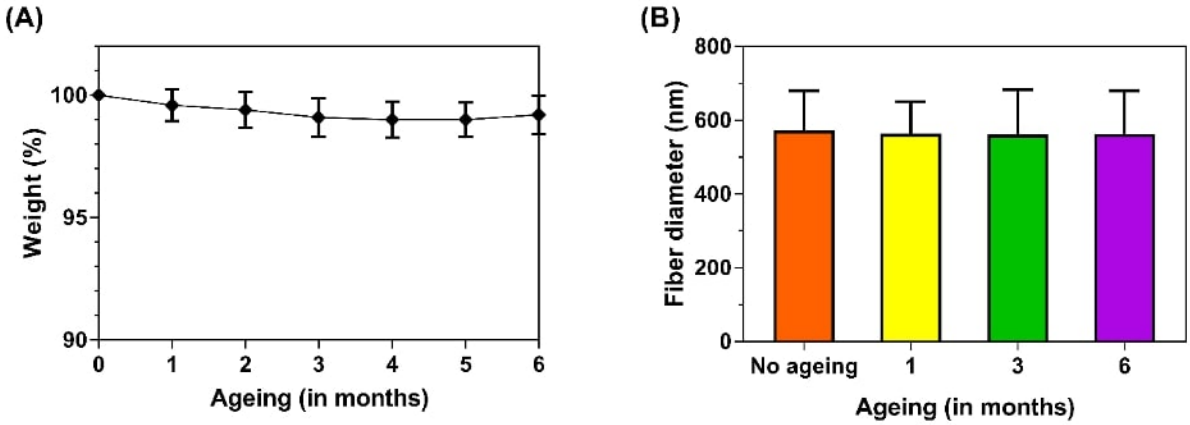

Figure A.1 - Measurements of (A) weight and (B) fiber diameter of the eVG scaffolds as a function of ageing duration in a saline solution at 37°C over 6 months (Mean+SD; n>60).

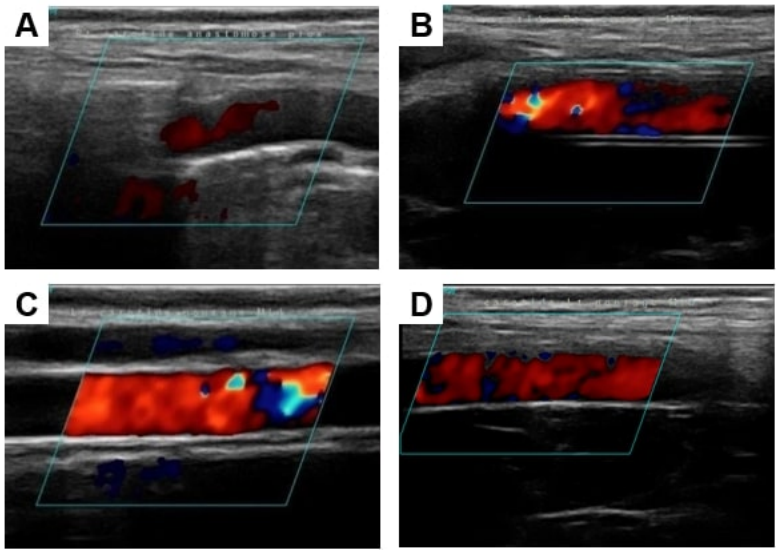

Figure A.2 - Doppler ultrasound images for ePTFE (A, B) and eVG-CS (C, D) grafts post-operatively (A, C) and 1 week after the implantation (B, D). All images taken at mid graft, except for (A) taken at proximal anastomosis because of the absence of Doppler signal inside the ePTFE prosthesis just after implantation.

APPENDIX B. Supplemental details on material and methods

B.1 Animal preoperative quarantine details

Animals were group housed in a room ventilated with filtered 100 % outside air (room temperature 19 +/- 1° C, relative humidity 50 +/-10 %). A 12-h: 12-h light: dark cycle was used. The animals had free access to good quality hay (Norfoin Inc., Saint-Césaire, QC, Canada) and water. The quantity of pelleted diet (Teklad Ruminant Diet 7060, Envigo, Madison, WI, USA) was limited to 250 ml/day. The animals were treated 5 days with fenbendazole per os (5 mg/kg, Safe-Guard Suspension, Merck Animal Health, Kirkland, QC, Canada) to control parasites.

B.2 Perioperative anesthesia protocol

On the day of the procedure the sheep received a premedication of butorphanol subcutaneously (SC) (0.05mg/kg Torbugesic® Zoetis Canada Inc., Kirkland, QC, Canada). A 20 G catheter (Jelco, Smiths Medical ASD, Inc., Southington, CT, USA) was introduced in the cephalic vein and general anesthesia was induced with an intravenous (IV) injection of diazepam (0.2mg/kg, Diazepam injection USP, Sandoz, Boucherville, QC, Canada) and ketamine (2mg/kg Ketalean Bimeda-MTC Animal Health Inc., Cambrige, ON, Canada). Endotracheal intubation was performed with a 8.5 mm (ID) cuffed endotracheal tube (Teleflex, Research Triangle Park, NC, USA) and anesthesia was maintained with isoflurane (2-3 %, Forane, Baxter, Mississauga, ON, Canada) and a FiO2 of 1. Intermittent positive pressure ventilation (Ohio 7000, Omeda, Rexdale, ON, Canada) was use and ventilation parameters were adjusted to maintain the end-tidal carbon dioxide concentration (EtPCO2) between 35 and 45 mmHg. A positive end-expiratory pressure (PEEP) was maintained with a 5 cm H2O PEEP valve (Hallowell EMC, Pittsfield, MA, USA) installed on the expiratory limb of the circle system. An orogastric tube (Stomach Tube, JorVet, McCarthy & Sons Service, Calgary, AB, Canada) was used to prevent free gas bloat.

To ensure preemptive analgesia the animal received an IV bolus of ketamine (0.2 mg/kg), fentanyl (0.005 mg/kg, Sandoz, Boucherville, QC, Canada) and lidocaine hydrochloride (1 mg/kg, Hospira, Montreal, QC, Canada) followed by constant rate infusion (CRI) of ketamine (0.3 mg/kg/h), fentanyl (0.005 mg/kg/h) and lidocaine (1.5 mg/kg/h). The surgical site was infiltrated with bupivacaine hydrochloride (2 mg/kg, Marcaine, Hospira, Montreal, QC, Canada). The animal also received IV Meloxicam (0.5 mg/kg, Metacam, Boehringer Ingelheim Ltd., Burlington, ON, Canada) and SC buprenorphine (0.005 mg/kg, Vetergesic®, Sogeval UK Limited, Sheriff Hutton York, UK) 1 hour prior to the surgical procedure. Cefazolin was administered IV (22 mg/k, Hospira, Montreal, QC, Canada), at the beginning of the surgical procedure to prevent microbiological infection.

To ensure postoperative analgesia a fentanyl transdermal patch (1.5 µg/kg, Mylan Pharmaceutical ULC, Etobicoke, ON, Canada) was placed at the beginning of the anesthesia and removed 72 hours later. Post-operative analgesia was also provided for 3 days with daily meloxicam per os (1 mg/kg, Meloxicam oral suspension Solvet Alberta Veterinary Laboratories, Calgary, AB, Canada).

B.3 Sedation protocol for echographic follow-up

The echography was performed under butrophanol sedation (0.05mg/kg Torbugesic, Zoetis Canada Inc., Kirkland, QC, Canada).

REFERENCES

[1] D. Lloyd-Jones, R.J. Adams, T.M. Brown, M. Carnethon, S. Dai, G. De Simone, T.B. Ferguson, E. Ford, K. Furie, C. Gillespie, A. Go, K. Greenlund, N. Haase, S. Hailpern, P.M. Ho, V. Howard, B. Kissela, S. Kittner, D. Lackland, L. Lisabeth, A. Marelli, M.M. McDermott, J. Meigs, D. Mozaffarian, M. Mussolino, G. Nichol, V.L. Roger, W. Rosamond, R. Sacco, P. Sorlie, R. Stafford, T. Thom, S. Wasserthiel-Smoller, N.D. Wong, J. Wylie-Rosett, Heart disease and stroke statistics - 2010 update: A report from the American heart association, Circulation 121(7) (2010) 948-954.

[2] L. Norgren, W.R. Hiatt, J.A. Dormandy, M.R. Nehler, K.A. Harris, F.G.R. Fowkes, Inter-Society Consensus for the Management of Peripheral Arterial Disease (TASC II), J. Vasc. Surg. 45(1 Suppl.) (2007) S5-S67.

[3] G.L. Londrey, D.E. Ramsey, K.J. Hodgson, L.D. Barkmeier, D.S. Sumner, Infrapopliteal bypass for severe ischemia: Comparison of autogenous vein, composite, and prosthetic grafts, J. Vasc. Surg. 13(5) (1991) 631-636.

[4] F.J. Veith, S.K. Gupta, E. Ascer, S. White-Flores, R.H. Samson, L.A. Scher, J.B. Towne, V.M. Bernhard, P. Bonier, W.R. Flinn, P. Astelford, J.S.T. Yao, J.J. Bergan, Six-year prospective multicenter randomized comparison of autologous saphenous vein and expanded polytetrafluoroethylene grafts in infrainguinal arterial reconstructions, J. Vasc. Surg. 3(1) (1986) 104-114.

[5] F.W. Hehrlein, M. Schlepper, F. Loskot, H.H. Scheld, P. Walter, J. Mulch, The use of expanded polytetrafluoroethylene (PTFE) grafts for myocardial revascularization, J. Cardiovasc. Surg. 25(6) (1984) 549-553.

[6] P. Zilla, D. Bezuidenhout, P. Human, Prosthetic vascular grafts: Wrong models, wrong questions and no healing, Biomaterials 28 (2007) 5009-5027.

[7] M. Albers, V.M. Battistella, M. Romiti, A.A. Eyer Rodrigues, C.A. Bragança Pereira, Meta-analysis of polytetrafluoroethylene bypass grafts to infrapopliteal arteries, J. Vasc. Surg. 37(6) (2003) 1263-1269.

[8] O.E. Teebken, A. Haverich, Tissue engineering of small diameter vascular grafts, Eur. J. Vasc. Endovasc. Surg. 23(6) (2002) 475-485.

[9] M.S. Baguneid, A.M. Seifalian, H.J. Salacinski, D. Murray, G. Hamilton, M.G. Walker, Tissue engineering of blood vessels, Br. J. Surg. 93(3) (2006) 282-290.

[10] S. Pashneh-Tala, S. MacNeil, F. Claeyssens, The Tissue-Engineered Vascular Graft-Past, Present, and Future, Tissue Eng. Part B Rev. 22(1) (2016).

[11] D.G. Seifu, A. Purnama, K. Mequanint, D. Mantovani, Small-diameter vascular tissue engineering, Nat. Rev. Cardiol. 10 (2013) 410.

[12] R. Botting, J.R. Vane, Mediators and the anti-thrombotic properties of the vascular endothelium, Ann. Med. 21(1) (1989) 31-38.

[13] M.W. Radomski, R.M.J. Palmer, S. Moncada, The anti-aggregating properties of vascular endothelium: interactions between prostacyclin and nitric oxide, Br. J. Pharmacol. 92(3) (1987) 639-646.

[14] A. Sandoo, J.J.C.S.V. van Zanten, G.S. Metsios, D. Carroll, G.D. Kitas, The endothelium and its role in regulating vascular tone, Open Cardiovasc. Med. J. 4 (2010) 302-312.

[15] A.W. Clowes, T.R. Kirkman, M.A. Reidy, Mechanisms of arterial graft healing. Rapid transmural capillary ingrowth provides a source of intimal endothelium and smooth muscle in porous PTFE prostheses, Am. J. Pathol. 123(2) (1986) 220-230.

[16] N.R. Tai, H.J. Salacinski, A. Edwards, G. Hamilton, A.M. Seifalian, Compliance properties of conduits used in vascular reconstruction, Br. J. Surg. 87(11) (2000) 1516-1524.

[17] W.M. Abbott, A. Callow, W. Moore, R. Rutherford, F. Veith, S. Weinberg, Evaluation and performance standards for arterial prostheses, J. Vasc. Surg. 17(4) (1993) 746-756.

[18] M.J. Collins, X. Li, W. Lv, C. Yang, C.D. Protack, A. Muto, C.C. Jadlowiec, C. Shu, A. Dardik, Therapeutic strategies to combat neointimal hyperplasia in vascular grafts, Expert Rev. Cardiovasc. Ther. 10(5) (2012) 635-647.

[19] K.A. Rocco, M.W. Maxfield, C.A. Best, E.W. Dean, C.K. Breuer, In vivo applications of electrospun tissue-engineered vascular grafts: A review, Tissue Eng. Part B Rev. 20(6) (2014) 628-640.

[20] A. Hadjizadeh, A. Ajji, M.N. Bureau, Nano/micro electro-spun polyethylene terephthalate fibrous mat preparation and characterization, J. Mech. Behav. Biomed. Mater. 4(3) (2011) 340-51.

[21] A. Hadjizadeh, A. Ajji, M. Jolicoeur, B. Liberelle, G. De Crescenzo, Effects of Electrospun Nanostructure versus Microstructure on Human Aortic Endothelial Cell Behavior, J. Biomed. Nanotechnol. 9 (2013) 1159-1209.

[22] H. Savoji, A. Hadjizadeh, M. Maire, A. Ajji, M.R. Wertheimer, S. Lerouge, Electrospun nanofiber scaffolds and plasma polymerization: a promising combination towards complete, stable endothelial lining for vascular grafts, Macromol. Biosci. 14(8) (2014) 1084-1095.

[23] P.K. Thalla, H. Fadlallah, B. Liberelle, P. Lequoy, G. De Crescenzo, Y. Merhi, S. Lerouge, Chondroitin sulfate coatings display low platelet but high endothelial cell adhesive properties favorable for vascular implants, Biomacromolecules 15(7) (2014) 2512-20.

[24] H. Savoji, M. Maire, P. Lequoy, B. Liberelle, G. De Crescenzo, A. Ajji, M.R. Wertheimer, S. Lerouge, Combining Electrospun Fiber Mats and Bioactive Coatings for Vascular Graft Prostheses, Biomacromolecules 18(1) (2017) 303-310.

[25] M. Bouchet, M. Gauthier, M. Maire, A. Ajji, S. Lerouge, Towards Compliant Small-Diameter Vascular Grafts: Predictive Analytical Model and Experiments, Mater. Sci. Eng. C 100 (2019) 715-723.

[26] F. Guo, N. Wang, L. Wang, L. Hou, L. Ma, J. Liu, Y. Chen, B. Fan, Y. Zhao, An electrospun strong PCL/PU composite vascular graft with mechanical anisotropy and cyclic stability, J. Mater. Chem. A 3(9) (2015) 4782-4787.

[27] F. Montini-Ballarin, G.A. Abraham, P.C. Caracciolo, Mechanical Behavior of Polyurethane-Based Small-Diameter Vascular Grafts, in: S.L. Cooper, J. Guan (Eds.), Advances in Polyurethane Biomaterials, Woodhead Publishing,2016, pp. 451-477.

[28] C. Charbonneau, B. Liberelle, M.-J. Hébert, G. De Crescenzo, S. Lerouge, Stimulation of cell growth and resistance to apoptosis in vascular smooth muscle cells on a chondroitin sulfate/epidermal growth factor coating, Biomaterials 32(6) (2011) 1591-1600.

[29] American National Standards Institute, ANSI/AAMI/ISO 7198:1998/2001/(R)2010, Cardiovascular implants - Tubular vascular prostheses, Association for the Avancement of Medical Instrumentation, 2010, p. 56.

[30] ASTM International, ASTM D882-12, Standard Test Method for Tensile Properties of Thin Plastic Sheeting, 2012, p. 11.

[31] A. Kónya, K.C. Wright, M. Gounis, K. Kandarpa, Animal Models for Atherosclerosis, Restenosis, and Endovascular Aneurysm Repair, in: P.M. Conn (Ed.), Sourcebook of Models for Biomedical Research, Humana Press, Totowa, NJ, 2008, pp. 369-384.

[32] C. Kilkenny, W.J. Browne, I.C. Cuthill, M. Emerson, D.G. Altman, Improving Bioscience Research Reporting: The ARRIVE Guidelines for Reporting Animal Research, PLoS Biol. 8(6) (2010) e1000412.

[33] P.F. Sánchez, E.M. Brey, J.C. Briceño, Endothelialization mechanisms in vascular grafts, J. Tissue Eng. Regen. Med. 12(11) (2018) 2164-2178.

[34] P. Lequoy, H. Savoji, B. Saoudi, A. Bertrand-Grenier, M.R. Wertheimer, G. De Crescenzo, G. Soulez, S. Lerouge, In Vitro and Pilot in Vivo Evaluation of a Bioactive Coating for Stent Grafts Based on Chondroitin Sulfate and Epidermal Growth Factor, J. Vasc. Intervent. Radiol. 27(5) (2016) 753-760e3.

[35] M.J. Moreno, A. Ajji, D. Mohebbi-Kalhori, M. Rukhlova, A. Hadjizadeh, M.N. Bureau, Development of a compliant and cytocompatible micro-fibrous polyethylene terephthalate vascular scaffold, J. Biomed. Mater. Res. B 97(2) (2011) 201-214.

[36] Y. Chen, X. Ding, Y.L. Li, X.Q. Zhao, J.Y. Hu, Experimental Models of Compliance and Young's Modulus of Woven Vascular Prosthesis, Adv. Mater. Res. 332-334 (2011) 609-612.

[37] K. Billiar, J. Murray, D. Laude, G. Abraham, N. Bachrach, Effects of carbodiimide crosslinking conditions on the physical properties of laminated intestinal submucosa, J. Biomed. Mater. Res. 56(1) (2001) 101-108.

[38] H. Rostad, A. Grip, C. Hall, Blood flow measurement in PTFE grafts, J. Cardiovasc. Surg. 28(3) (1987) 262-265.

[39] D. Mantovani, M. Castonguay, J.F. Pageau, M. Fiset, G. Laroche, Ammonia RF-Plasma Treatment of Tubular ePTFE Vascular Prostheses, Plasmas Polym. 4(2) (1999) 207-228.

[40] M. Laurent, Utilisation d'une décharge à barrière diélectrique pour développer une matrice polymère plasma dégradable pour des applications vasculaires, Doctoral dissertation, Université Laval, Québec, 2017, p. 226.

[41] Y. Zhu, C. Gao, T. He, J. Shen, Endothelium regeneration on luminal surface of polyurethane vascular scaffold modified with diamine and covalently grafted with gelatin, Biomaterials 25(3) (2004) 423-430.

[42] Y. Zhu, C. Gao, X. Liu, J. Shen, Surface Modification of Polycaprolactone Membrane via Aminolysis and Biomacromolecule Immobilization for Promoting Cytocompatibility of Human Endothelial Cells, Biomacromolecules 3(6) (2002) 1312-1319.

[43] S.J. Lee, J. Liu, S.H. Oh, S. Soker, A. Atala, J.J. Yoo, Development of a composite vascular scaffolding system that withstands physiological vascular conditions, Biomaterials 29(19) (2008) 2891-8.

[44] Z. Niu, X. Wang, X. Meng, X. Guo, Y. Jiang, Y. Xu, Q. Li, C. Shen, Controllable fiber orientation and nonlinear elasticity of electrospun nanofibrous small diameter tubular scaffolds for vascular tissue engineering, Biomed. Mater. 14(3) (2019) 035006.

[45] J. Fernández, O. Auzmendi, H. Amestoy, A. Diez-Torre, J.-R. Sarasua, Mechanical properties and fatigue analysis on poly(ε-caprolactone)-polydopamine-coated nanofibers and poly(ε-caprolactone)-carbon nanotube composite scaffolds, Eur. Polym. J. 94 (2017) 208-221.

[46] Y.M. Ju, J.S. Choi, A. Atala, J.J. Yoo, S.J. Lee, Bilayered scaffold for engineering cellularized blood vessels, Biomaterials 31(15) (2010) 4313-21.

[47] B.M. Whited, M.N. Rylander, The influence of electrospun scaffold topography on endothelial cell morphology, alignment, and adhesion in response to fluid flow, Biotechnol. Bioeng. 111(1) (2014) 184-195.

[48] S. Soliman, S. Sant, J.W. Nichol, M. Khabiry, E. Traversa, A. Khademhosseini, Controlling the porosity of fibrous scaffolds by modulating the fiber diameter and packing density, J. Biomed. Mater. Res. A 96(3) (2011) 566-74.

[49] Z. Zhang, Z. Wang, S. Liu, M. Kodama, Pore size, tissue ingrowth, and endothelialization of small-diameter microporous polyurethane vascular prostheses, Biomaterials 25(1) (2004) 177-187.

[50] T. Pennel, D. Bezuidenhout, J. Koehne, N.H. Davies, P. Zilla, Transmural capillary ingrowth is essential for confluent vascular graft healing, Acta Biomater. 65 (2018) 237-247.

[51] Z.J. Hu, Z.L. Li, L.Y. Hu, W. He, R.M. Liu, Y.S. Qin, S.M. Wang, The in vivo performance of small-caliber nanofibrous polyurethane vascular grafts, BMC Cardiovasc. Disord. 12 (2012).

[52] T. Pennel, P. Zilla, D. Bezuidenhout, Differentiating transmural from transanastomotic prosthetic graft endothelialization through an isolation loop-graft model, J. Vasc. Surg. 58(4) (2013) 1053-1061.

[53] R.A. White, The effect of porosity and biomaterial on the healing and long-term mechanical properties of vascular prostheses, ASAIO Transactions 34(2) (1988) 95-100.

[54] J. Pu, F. Yuan, S. Li, K. Komvopoulos, Electrospun bilayer fibrous scaffolds for enhanced cell infiltration and vascularization in vivo, Acta Biomater. (2014).

[55] N. Jirofti, D. Mohebbi-Kalhori, A. Samimi, A. Hadjizadeh, G.H. Kazemzadeh, Small-diameter vascular graft using co-electrospun composite PCL/PU nanofibers, Biomedical Materials (2018).

[56] M. Bode, M. Mueller, H. Zernetsch, B. Glasmacher, Electrospun vascular grafts with anti-kinking properties: Development of a method to optimize the bendability of electrospun vascular grafts and of a standardized flow-bending test method. Current Directions in Biomedical Engineering, 1(1) (2015) 524-528.

[57] Z. Tan, H. Wang, X. Gao, T. Liu, & Y. Tan, Composite vascular grafts with high cell infiltration by co-electrospinning. Materials Science and Engineering: C (2016), 67, 369-377.

[58] M. Rahmani, M. M. Khani, S. Rabbani, A. Mashaghi, F. Noorizadeh, R. Faridi-Majidi, & H. Ghanbari, Development of poly (mannitol sebacate)/poly (lactic acid) nanofibrous scaffolds with potential applications in tissue engineering. Materials Science and Engineering: C (2020), 110, 110626.